JOURNAL OF VIROLOGY, July 2005, p. 8625–8628 Vol. 79, No. 13
0022-538X/05/$08.00+0 doi:10.1128/JVI.79.13.8625–8628.2005

Real-Time Detection of Virus Particles and Viral Protein Expression with Two-Color Nanoparticle Probes

Amit Agrawal,[1] Ralph A. Tripp,[2]* Larry J. Anderson,[3] and Shuming Nie[1]*

Departments of Biomedical Engineering and Chemistry, Emory University and Georgia Institute of Technology, 1639 Pierce Drive, Suite 2001,[1] and Centers for Disease Control and Prevention, National Center for Infectious Diseases, Division of Respiratory and Enteric Viruses,[3] Atlanta, and College of Veterinary Medicine, Department of Infectious Diseases, University of Georgia, Athens,[2] Georgia

Received 3 November 2004/Accepted 17 February 2005

Respiratory syncytial virus (RSV) mediates serious lower respiratory tract illness in infants and young children and is a significant pathogen of the elderly and immune compromised. Rapid and sensitive RSV diagnosis is important to infection control and efforts to develop antiviral drugs. Current RSV detection methods are limited by sensitivity and/or time required for detection. In this study, we show that antibody-conjugated nanoparticles rapidly and sensitively detect RSV and estimate relative levels of surface protein expression. A major development is use of dual-color quantum dots or fluorescence energy transfer nanobeads that can be simultaneously excited with a single light source.

Respiratory syncytial virus (RSV) is the most important cause of serious lower respiratory tract illness in infants and young children worldwide, causing repeat infections throughout life, and RSV may cause serious complications in the elderly and immune compromised patients (1, 4–6, 8, 11, 14, 15). RSV generally initiates mild upper respiratory tract infection in young children, with infection rates approaching 50% in the first year of life (9); however, up to 40% of infected children develop serious lower respiratory tract disease, with a substantial number of patients requiring hospitalization (10, 14). No safe and effective RSV vaccine is available, but immunoprophylaxis is available for certain high-risk infants, and strict attention to good infection control practices may prevent nosocomial RSV infection. The availability of sensitive diagnostics can signal the need to implement infection control and guide the timing of immunoprophylaxis and may be used to guide RSV antiviral treatment.

RSV diagnostics for patient management needs to be sensitive, specific, and rapid, requiring direct detection of virus, viral antigens, or RNA, usually in nasopharyngeal specimens. RSV isolation in cell culture has been considered the reference method, followed by immunofluorescence assay or enzyme immunosorbent assay; however, results from virus isolation studies are not rapidly available for patient management, and immunofluorescence assay and enzyme immunosorbent assay are not sufficiently sensitive to detect infection in a substantial portion of patients. Serological studies require seroconversion and thus cannot be completed during the acute illness, and PCR assays may be affected by template contamination and false-positive results. We developed nanotechnology based on the principles of microcapillary flow cytometry and single-molecule detection (2, 12) to detect RSV rapidly and with high sensitivity. We used two types of fluorescent nanoparticles: (i) 40-nm carboxylate-modified fluorescent nanoparticles (G nanoparticles, 505/515; R nanoparticles, 488/685; Molecular Probes Inc.) and (ii) streptavidin-coated Quantum Dots (QDs, 488/605; QDC Corp.) (3). The microcapillary flow system is integrated with a fixed-point confocal microscope with a high-numerical-aperture 100× objective. At low concentrations, the photons emitted from the nanoparticles in the confocal probe volume (~2 fl) are spectrally separated and analyzed for coincidence of time of arrival at two avalanche photodiodes (13). To detect RSV, 40-nm fluorescent nanoparticles were coupled to either anti-RSV F protein (clone 131-2A; Chemicon International, Temecula, CA) or anti-RSV G protein (clone 130-2G; Chemicon) monoclonal antibodies (16) and allowed to interact with RSV, and the photons produced by laser excitation of the fluorophores passing through the confocal probe volume were detected in real time. The system operates on the concept that if two nanoparticles are free to move in a solution, photons generated by them will arrive at the detector at different times unless they are bound to the same target. This concept can be used to detect target molecules at low concentrations with high sensitivity and discriminate between aggregate particles. Traditional fluorescent dyes are less suitable as labels because they require excitation at two different wavelengths, making it difficult to ensure that all photon signals are generated from the same probe volume. QDs and FRET nanoparticles used in this system are better suited because they can be excited at the same wavelength while emitting at different

* Corresponding author. Mailing address for Ralph A. Tripp: College of Veterinary Medicine, Department of Infectious Diseases, University of Georgia, Athens, GA 30602. Phone: (706) 542-1557. Fax: (706) 583-0176. E-mail: ratripp@uga.edu. Mailing address for Shuming Nie: Departments of Biomedical Engineering and Chemistry, Emory University and Georgia Institute of Technology, 1639 Pierce Drive, Suite 2001, Atlanta, GA 30322. Phone: (404) 712-8595. Fax: (404) 727-9873. E-mail: snie@emory.edu.

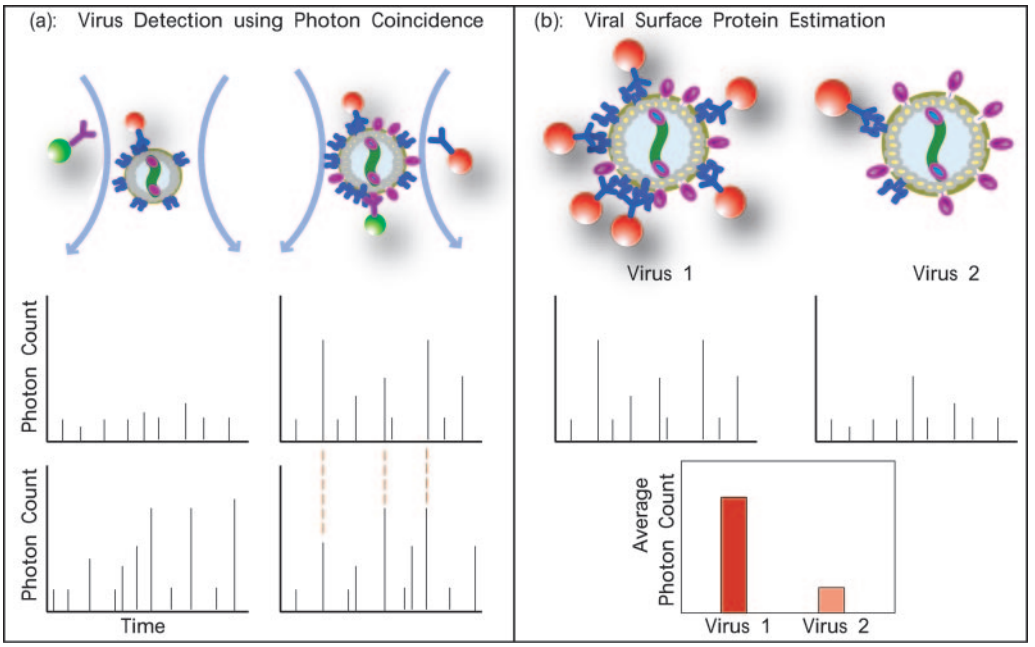

FIG. 1. Schematic illustration of single-virus detection and surface protein determination. A virus bound with complementary nanoparticle-antibody probes flows into a confocal volume (confined by blue lines), where fluorescent nanoparticles are excited by a laser. The photons from green and red fluorescent nanoparticles are separated (spectra at the bottom) and analyzed for time correlation (coincidence). (a) The virus that does not bind to both probes (left) will not show coincidence signals (dotted lines), while the virus that binds to both probes (right) will produce time-correlated photons from the red and green detection channels. (b) When a single-color probe is used, the virus that binds to several probes (virus 1) will exhibit greater intensity in the integrated photon count spectrum. The bottom graph shows the expected trend in average intensity calculated from several photon count spectra.

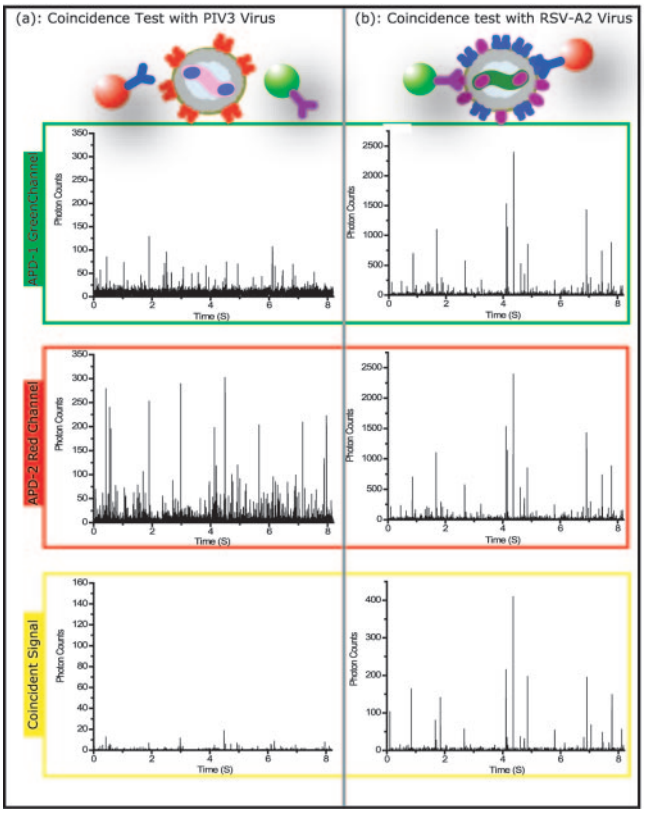

FIG. 2. Time-correlated coincidence signals for virus detection in solution. Forty-nanometer nanoparticles conjugated to RSV anti-F or anti-G protein monoclonal antibodies were used to produce red or green photon emission, respectively. PIV3, used as a control, produced low red or green photon counts and did not show coincidence signals (a), while coincident peaks were observed for the RSV/A2 (b). The time for detection was 8 s, and signals were acquired and analyzed in real time (without any delay).

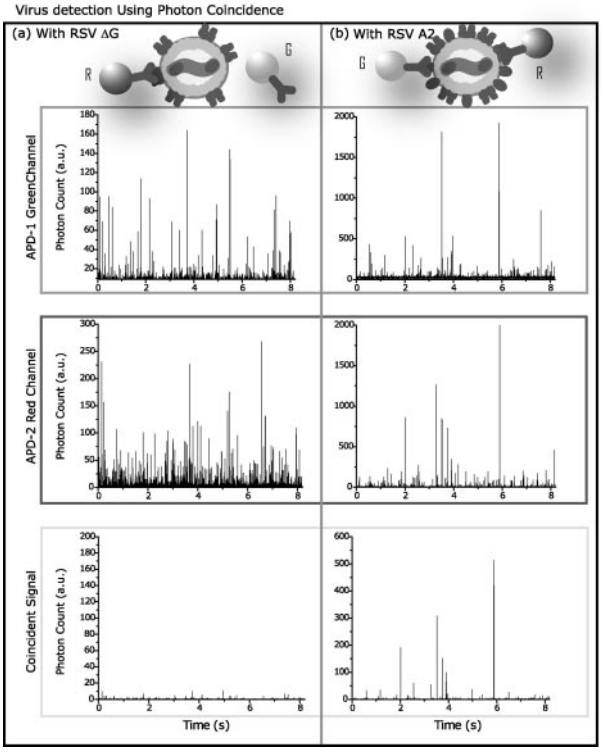

FIG. 3. Time-correlated coincidence signals for virus detection in solution. Forty-nanometer nanoparticles conjugated to RSV anti-F or anti-G protein monoclonal antibodies were used to produce red or green photon emission, respectively. RSVΔG, used as a control, produced low green photon counts, as expected, and did not show coincidence signals (a), while coincident peaks were observed for RSV/A2 (b). The magnitude of the red channel signal for RSVΔG was low compared to RSV/A2, suggestive of lower F protein expression compared to RSV/A2. The time for detection was 8 s, and signals were acquired and analyzed in real time (without any delay). a.u., arbitrary units.

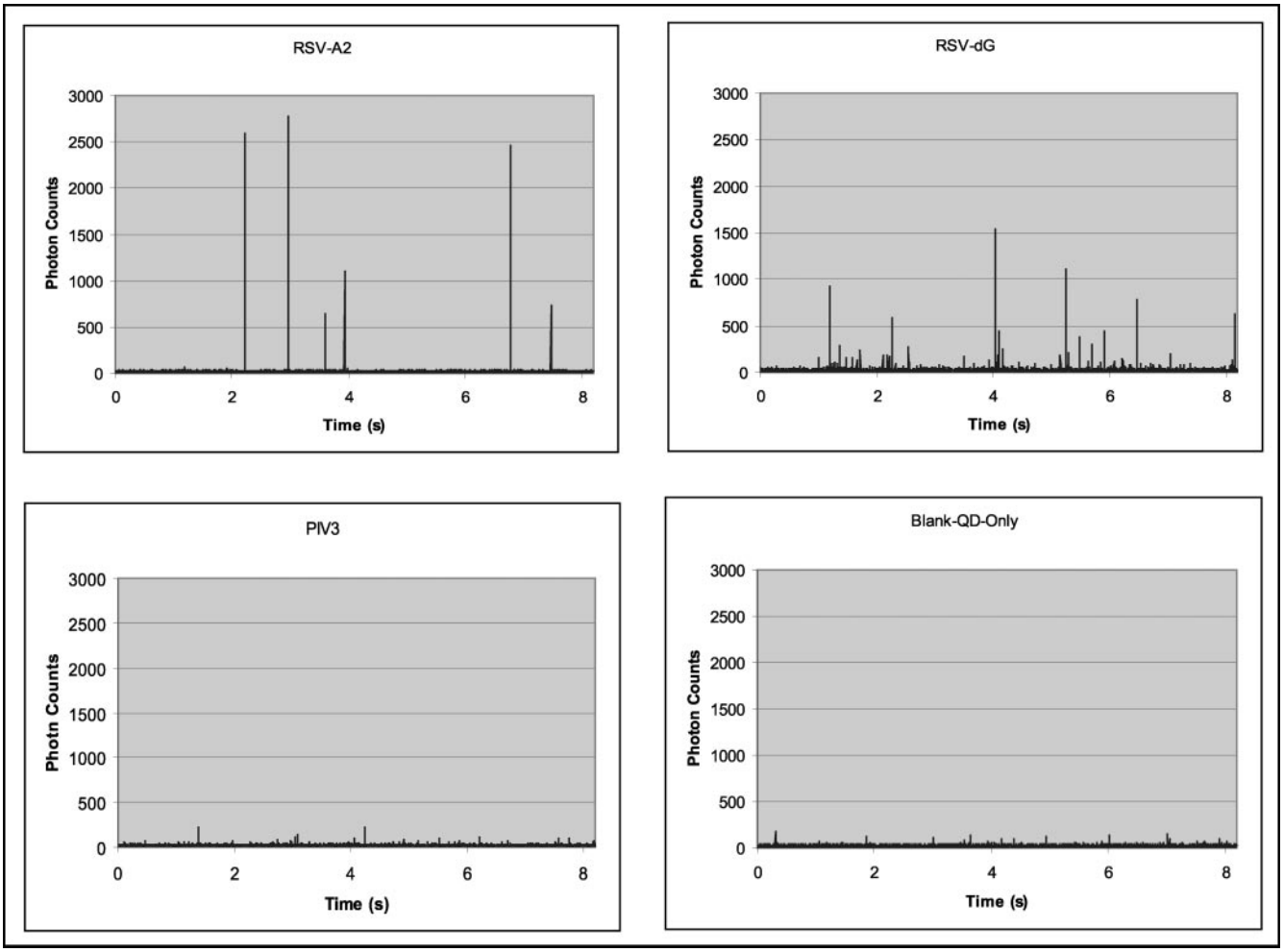

FIG. 4. Measurement of RSV F protein expression on virus particles. QDs coupled with anti-RSV F protein monoclonal antibody and incubated with different viruses generated different photon counts based on anti-F protein nanoparticle aggregation. No signal above the unconjugated QD control was observed for PIV3. Differences in the signal intensities obtained between RSV/A2 and RSVΔG are suggestive of differences in the level of F protein expression.

colors, allowing dual-color, time-correlated detection of single molecules and single virus particles.

To confirm the specificity of nanoparticle detection, we examined reactivity to uninfected Vero cell lysate, and sucrose density-purified viruses RSV/A2, RSVΔG (RSV mutant with G protein gene deletion), and parainfluenza virus type 3 (PIV3) propagated in Vero cells (17). Purified virus (10^5 PFU/ml) was incubated with R nanoparticles (anti-F protein) or G nanoparticles (anti-RSV G protein) as previously described (16). The microcapillary flow-based single-molecule detection system was used to detect very low levels and possibly single virus particles in solution based on the concept that at low concentrations of nanoparticles, coincident photons will be observed only if R and G nanoparticles bind to the same virus particle (Fig. 1a). A similar scheme was used to estimate relative amounts of virus surface protein expression (Fig. 1b); that is, if one type of virus particle has a higher level of protein expression on its surface, it is likely to bind more of that specific nanoparticle. Hence, the number of photons emitted in the same amount of time will be greater, resulting in higher

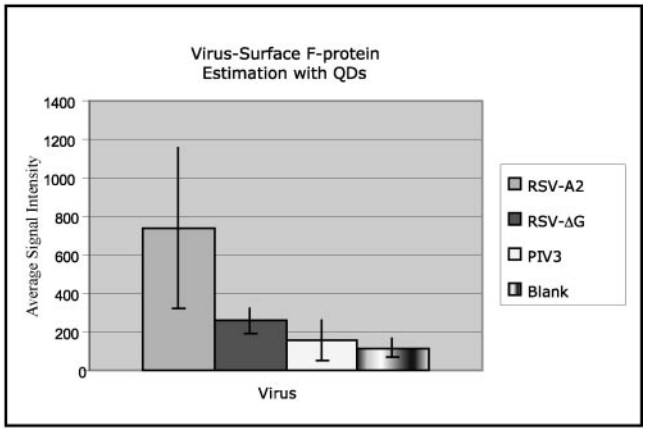

FIG. 5. Virus protein expression determined by average photon peak intensities. Photon counts were determined from 35 individual runs (8 s each) and averaged for each virus. The bars indicate the mean ± standard deviations.

intensity in the integrated photon count spectrum. This concept was used to compare the level of F protein expression on different RSV strains.

Figure 2 shows results obtained from photon coincidence experiments for virus particle detection. PIV3 was used as the negative control for nanoparticles conjugated to RSV F or G protein monoclonal antibodies. For PIV3, the photon count signal in both the red and green channels is low and there is no coincidence between the signals in the red and green channels (Fig. 2a). In contrast, for RSV/A2 viruses (Fig. 2b), there are substantial coincident signals in the red and green channels, confirming detection of virus particles. As an additional control, we examined the red and green channel signals for detection of RSVΔG (Fig. 3) and did not detect substantial green channel signals or red and green coincidence signals, indicating the high specificity of nanoparticle detection. The results in Fig. 2 also indicate that the intensity of photon count signals may be used to estimate the relative level of virus surface protein expression. The increase in photon counts in red and the green channels reflects the number of nanoparticles reactive with virus surface proteins and is independent of coincidence signals. Thus, the photon count in the red or green channel is lower for PIV3 and RSVΔG compared to RSV/A2 (Fig. 2 and Fig. 3).

Interestingly, lower levels of R nanoparticle aggregation were detected for RSVΔG compared to RSV/A2 (Fig. 3). This finding is noteworthy as sequential 3′-to-5′ transcription of the RSV genome is believed to result in higher levels of mRNA transcripts by genes most proximal to the 3′ promoter end (7); thus, higher levels of surface F protein expression might be anticipated by RSVΔG compared to RSV/A2. To address this result, we examined F protein expression on RSVΔG, RSV/A2, and PIV3 using anti-RSV F protein monoclonal antibodies conjugated to QDs at the same concentration used for R nanoparticle detection. A representative experiment of more than three separate experiments is shown in Fig. 4, and the average intensity of photon counts obtained from 35 runs (8 s each) is shown in Fig. 5. The intensity average was calculated after removing peaks below 100 counts so that signals from single QDs were eliminated. The average was calculated by dividing the total peak intensity by the total number of peaks. As shown in Fig. 4, and similar to the results obtained for R nanoparticles (Fig. 2 and Fig. 3), the hierarchy of peak intensity for QDs that react with RSV F protein is RSV/A2 $>$ RSVΔG $>$ PIV3 $\approx$ blank. It is possible that the lower level of F protein expression by RSVΔG compared to RSV/A2 may be associated with altered gene expression levels linked to changes in the gene end termination signal that precedes the F protein gene, as changes in this region may affect downstream gene expression levels (18).

In summary, we show that nanoparticles can be used to rapidly and sensitively detect virus particles and can be used to estimate the relative amount of surface F protein expression on RSV particles. These features may be useful in multiplexed applications for detecting and differentiating various viruses and other infectious agents in body fluid samples.

We acknowledge Rene Alvarez for help in virus preparation.

R.T. acknowledges the Georgia Research Alliance, which provided support for R. Alvarez. This work was supported in part by grants from the National Institutes of Health (grants R01 GM60562 and P20 GM072069 to S.N.) and from the Georgia Cancer Coalition (Distinguished Cancer Scholar awards to S.N.).

REFERENCES

1. **Anonymous.** 2002. Respiratory syncytial virus activity—United States, 2000-01 season. Morb. Mortal. Wkly. Rep. **51**:26–28.
2. **Castro, A., and J. G. Williams.** 1997. Single-molecule detection of specific nucleic acid sequences in unamplified genomic DNA. Anal. Chem. **69:**3915–3920.
3. **Chan, W. C. W., and S. M. Nie.** 1998. Quantum dot bioconjugates for ultrasensitive nonisotopic detection. Science **281:**2016–2018.
4. **Couch, R. B., J. A. Englund, and E. Whimbey.** 1997. Respiratory viral infections in immunocompetent and immunocompromised persons. Am. J. Med. **102**:2–9, 25–26.
5. **Falsey, A. R.** 1998. Respiratory syncytial virus infection in older persons. Vaccine **16:**1775–1778.
6. **Falsey, A. R., and E. E. Walsh.** 2000. Respiratory syncytial virus infection in adults. Clin. Microbiol. Rev. **13:**371–384.
7. **Fearns, R., and P. L. Collins.** 1999. Model for polymerase access to the overlapped L gene of respiratory syncytial virus. J. Virol. **73:**388–397.
8. **Glezen, W. P., S. B. Greenberg, R. L. Atmar, P. A. Piedra, and R. B. Couch.** 2000. Impact of respiratory virus infections on persons with chronic underlying conditions. JAMA **283:**499–505.
9. **Glezen, W. P., L. H. Taber, A. L. Frank, and J. A. Kasel.** 1986. Risk of primary infection and reinfection with respiratory syncytial virus. Am. J. Dis. Child. **140:**543–546.
10. **Hall, C. B.** 2001. Respiratory syncytial virus and parainfluenza virus. N. Engl. J. Med. **344:**1917–1928.
11. **Hall, C. B.** 1999. Respiratory syncytial virus: a continuing culprit and conundrum. J. Pediatr. **135:**2–7.
12. **Keller, R. A., W. P. Ambrose, A. A. Arias, H. Gai, S. R. Emory, P. M. Goodwin, and J. H. Jett.** 2002. Analytical applications of single-molecule detection. Anal. Chem. **74**:316a–324a.
13. **Li, H., D. Zhou, H. Browne, S. Balasubramanian, and D. Klenerman.** 2004. Molecule by molecule direct and quantitative counting of antibody-protein complexes in solution. Anal. Chem. **76:**4446–4451.
14. **Shay, D. K., R. C. Holman, R. D. Newman, L. L. Liu, J. W. Stout, and L. J. Anderson.** 1999. Bronchiolitis-associated hospitalizations among US children, 1980–1996. JAMA **282:**1440–1446.
15. **Staat, M. A.** 2002. Respiratory syncytial virus infections in children. Semin. Respir. Infect. **17:**15–20.
16. **Taylor, J. R., M. M. Fang, and S. Nie.** 2000. Probing specific sequences on single DNA molecules with bioconjugated fluorescent nanoparticles. Anal. Chem. **72:**1979–1986.
17. **Tripp, R. A., D. Moore, L. Jones, W. Sullender, J. Winter, and L. J. Anderson.** 1999. Respiratory syncytial virus G and/or SH protein alters Th1 cytokines, natural killer cells, and neutrophils responding to pulmonary infection in BALB/c mice. J. Virol. **73:**7099–7107.
18. **Wertz, G. W., and R. M. Moudy.** 2004. Antigenic and genetic variation in human respiratory syncytial virus. Pediatr. Infect. Dis. J. **23:**S19–S24.